RSC Advances

ROYAL SOCIETY OF CHEMISTRY

www.rsc.org/advances

Journal Name RSC Advances Dynamic Article Links ►

Cite this: DOI: 10.1039/c0xx00000x

www.rsc.org/xxxxxx

ARTICLE TYPE

Synthesis of Multifunctional Lipid-Polymer Conjugates: Application to the Elaboration of Bright Far-Red Fluorescent Lipid Probes

Salim Adjili,[a,b] Arnaud Favier,[a,b*] Julien Massin,[c] Yann Bretonnière,[c] William Lacour,[a,b] Yi-Chun Lin,[a,b] Elodie Chatre,[a] Christophe Place,[a] Cyril Favard,[d] Delphine Muriaux,[e‡] Chantal Andraud,[c] Marie-Thérèse Charreyre[a,b*]

Received (in XXX, XXX) Xth XXXXXXXXX 20XX, Accepted Xth XXXXXXXXX 20XX
DOI: 10.1039/b000000x

A new class of lipid-ended polymer conjugates presenting reactive sites regularly distributed along the polymer chain were synthesized using RAFT polymerization. The chosen modular approach enables to prepare different lipid families by tuning the nature of the phospholipid α-end, the molecular weight and the lateral functions of the polymer chain. The multiple activated ester functions of the conjugates can indeed be used for the efficient coupling of a great variety of amino-containing entities of interest. In this study, we elaborated original fluorescent lipid-polymer probes for optical microscopy by coupling along the chain a controlled number of chromophores emitting in the far-red where auto-fluorescence and light absorption by biological samples are limited. Water-soluble fluorescent lipid probes exhibiting an enhanced brightness were obtained. As a proof of concept, these probes were able to efficiently label the lipid bilayer of liposomes of various sizes. Such multifunctional lipid-ended polymers thus exhibit a great potential to functionalize model and natural lipid assemblies.

Introduction

Lipid-polymer conjugates are increasingly used in a wide range of (bio)applications, the major one being the development of nanomedecine delivery devices.[1] Hydrophilic polymer chains carrying a lipid at one chain-end (lipid-ended polymers, LEPs) are very useful to stabilize lipid self-assemblies such as supported bilayers and liposomes. The terminal lipid residue is anchored in the lipid bilayer while the polymer chain provides steric stabilization. In addition, the LEPs may also carry another entity of interest, generally located at the other chain-end, in order to display specific functionalities at the surface of the self-assemblies (*e.g.* bioactive molecules to improve targeting properties).[2–4]

PEGylated lipids, that are composed of a linear polyethylene glycol (PEG) – a hydrophilic, flexible and inert polymer – covalently bound to the polar head of a lipid, are by far the main family of LEPs encountered in the literature. PEGylated lipids improve the stability of liposomes which, when injected *in vivo*, show prolonged blood circulation and stealth properties (*i.e.* limited opsonization).[5–9] Moreover, a wide range of chemical functions can advantageously be introduced at the remaining lipid-PEG chain-end,[10–12] for instance to enable the coupling of a fluorophore.[13,14] However, lateral functionalization of PEG chains still remains a challenge and it is yet difficult to introduce various functions along the chain.

On the other hand, α-, ω- and α,ω-functionalized polymers, can now be synthesized through controlled radical polymerization (CRP) techniques.[15–18] However, very few articles report the synthesis of LEPs and they are exclusively dealing with homopolymers.[19–23] Among the various CRP techniques, RAFT polymerization is one of the most versatile for the development of (bio)conjugates.[24] Our group recently reported the synthesis of a lipid-functionalized RAFT agent (Lipid-CTA) that efficiently controlled the homopolymerization of an acrylamide derivative, *N*-acryloylmorpholine (NAM),[22] leading to polymers exhibiting similar properties compared to PEG. Such RAFT homopolymerization resulted in well-defined Lipid-P(NAM) conjugates with a controlled molecular weight (MW), a narrow MW distribution and, as confirmed by MALDI-ToF mass spectrometry, an intact lipid α-chain-end. In addition, these lipid-polymer conjugates were successfully used to stabilize LipoParticles assemblies in relatively high ionic strength aqueous solutions.

Yet, no LEPs carrying multiple lateral functionalities along the polymer chain (multifunctional LEP conjugates) were reported to date. However, such structures are highly desirable for numerous applications, since they would enable the coupling of various densities/types of entities and consequently to finely tune the properties of the lipid-polymer conjugates. In the present study, we designed modular LEPs exhibiting i) a well-defined structure (molecular weight, composition, microstructure and functionality), ii) a lipid of interest attached at the α-end of an hydrophilic backbone and iii) multiple reactive functions (Fig. 1, Top) regularly distributed along the polymer chain that are further used for the covalent coupling of a controlled number of entities of interest.

RAFT polymerization was used to synthesize LEPs bearing

numerous activated ester lateral functions, well-known for their ability to efficiently bind a large variety of amino-containing (bio)molecules.[25,26] The reactive lipid-polymer backbone was synthesized in the presence of a Lipid-CTA, by copolymerization of NAM with *N*-acryloxysuccinimide (NAS), a comonomer pair leading to an excellent control over the architecture of the P(NAM-*co*-NAS) chains in terms of molecular weight (MW), dispersity but also composition and microstructure.[27] Indeed, we previously showed that RAFT copolymerization of NAM and NAS exhibits an azeotropic composition (NAM/NAS 60/40 mol%) for which there is no compositional drift throughout the polymerization (the co-monomer conversion kinetics are identical). Not only is the microstructure identical from one chain to another – which is inherent to a living copolymerization – but the activated ester units are regularly spaced along the polymer chain.

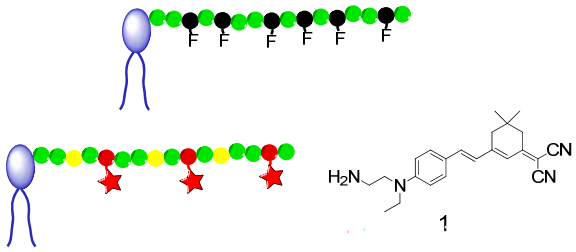

Fig. 1 Schematic representation of a multifunctional reactive lipid-ended polymers, LEPs, (top) that were used for the elaboration of fluorescent lipid-polymer probes (bottom, left) labeled with chromophore **1** (bottom, right). (NAM units – green, NAS units – black, F – reactive lateral functions, fluorophores – red stars).

Among the numerous potential applications of this multifunctional LEP platform, one particular interest in the field of bioimaging is the development of bright fluorescent lipid probes. Fluorescent lipids are used to label natural and/or artificial lipid bilayers such as liposomes.[28] For the synthesis of fluorescent lipids, hydrophobic fluorophores are most of the time introduced as part of the fatty acid chains. However, since the bulky and rigid structure of the fluorophore (compared to the natural fatty acids) may alter the insertion properties of the fluorescent lipid into the bilayers, introduction of the fluorophore on the polar head of the lipid may be preferred. In the latter case, a more hydrophilic fluorophore is either directly attached to the polar head or via a PEG linker.[13,29–31]
Conventional fluorescent lipids, including those commercially available, generally bear only one fluorophore leading to a moderate brightness. Our objective here was to develop fluorescent lipid-polymer probes bearing multiple fluorophores, thus exhibiting an enhanced brightness. The multifunctional LEP platform was therefore used for the covalent coupling of a controlled number of fluorophores along the hydrophilic polymer backbone (Fig. 1, bottom). We selected a push-pull dipolar fluorophore (Fig. 1) emitting in the far-red with interesting two-photon absorption properties. This class of chromophores (derivatives of isophorone) indeed exhibits many advantages for bioimaging applications since, at these operating wavelengths, light absorption and scattering by the biological tissues are low. As a consequence, phototoxicity and auto-fluorescence are reduced, while light penetration into tissues is higher.[32,33] This chromophore has recently been used for the elaboration of a water-soluble probe for cerebral vascular imaging.[34] It also presents an intense fluorescence in the aggregated state:[35] its fluorescence should then be less sensitive to the self-quenching phenomenon expected when multiple fluorophores are bound to the same polymer backbone.

As a proof of concept, several multifunctional LEP conjugates carrying a dipalmitoyl phospholipid at their α-chain-end and exhibiting various chain lengths were synthesized. Then, covalent coupling of the fluorophores along the chain was carried out, resulting in fluorescent LEP conjugates. In addition, the modularity of the multifunctional LEP platform was also used to introduce electrostatic charges that are known to influence the behavior of polymers under bio-relevant conditions. A library of neutral and negatively charged fluorescent LEP conjugates was prepared by varying the polymer molecular weight and the number of fluorophores per polymer chain. After purification, the photophysical properties of the conjugates were investigated using UV-Vis and fluorescence spectroscopies. Finally, optical microscopy was used to assess the ability of the new lipid-polymer probes to label model lipid bi-layers such as liposomes.

Results and Discussion

Synthesis and characterization of well-defined multifunctional LEPs

In a first step, Lipid-CTAs were synthesized (Scheme 1) from two dipalmitoyl phospholipids carrying a primary amino group, following the general strategy previously described.[22] Both lipid-CTAs, **A** and **B** (Fig. 2), are derivatives of 1,2-dipalmitoyl-*sn*-glycero-3-phosphoethanolamine (DPPE) but the newly synthesized one, **B**, differed from **A** by the absence of the C-6 spacer between the dithiobenzoate group and the phosphate of the lipid polar head. The structure of **B** was confirmed by both ^{1}H NMR spectroscopy (Fig. S1 in Electronic Supplementary Information) and mass spectrometry analyses.

It has to be noted that purification was improved at various levels compared to the previously described procedure (see also Experimental Section): i) Purification of the CAEDB derivative was facilitated by introducing an extraction step to isolate the product before silica gel chromatography which was then easier to conduct and more efficient. ii) Purity of the SEDB RAFT agent precursor was enhanced by a re-cristallization procedure, that led to a pink powder with a very high purity (>95%). This powder was much easier to handle than the oil generally obtained without re-crystallization. iii) Such SEDB purity facilitated the synthesis and the purification of the amphiphilic Lipid-CTAs. For the latter purification, the silica gel chromatography was advantageously replaced by a silica gel filtration in order to remove the residual salts arising from the extraction procedure. Finally, the two Lipid-CTAs were obtained with a 90% yield (>90% purity) relative to the initial phospholipid.

Cite this: DOI: 10.1039/c0xx00000x

www.rsc.org/xxxxxx

ARTICLE TYPE

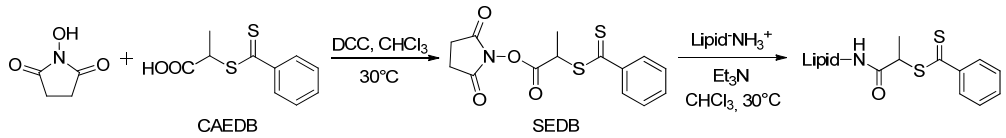

Scheme 1 General synthesis of the Lipid-CTAs

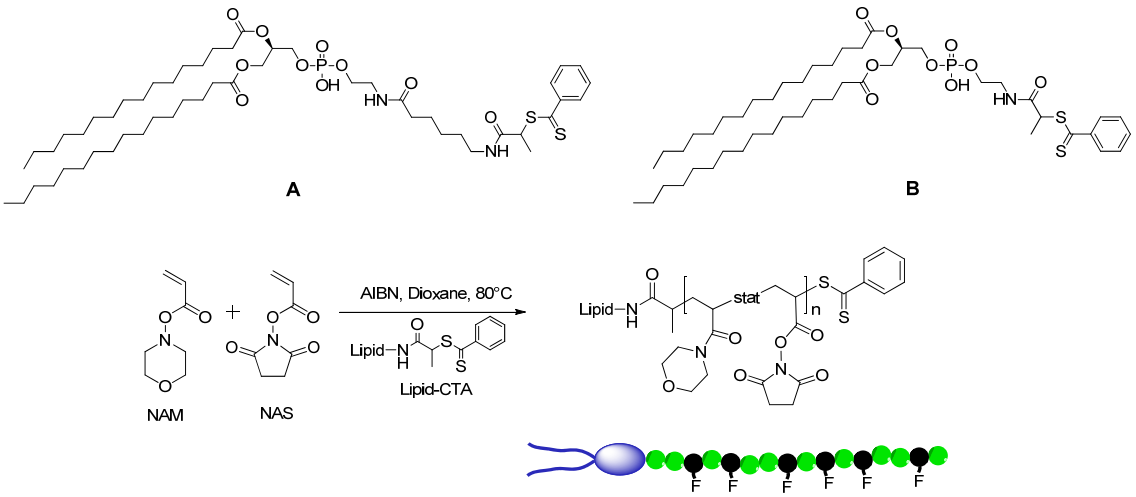

Fig. 2 The two Lipid-CTAs based on DPPE used in this study (top) to control the RAFT copolymerization of NAM and NAS (bottom)

The Lipid-CTAs were then used as control agents for the RAFT copolymerization of NAM and NAS. No influence of the presence of NAS in the co-monomer mixture and of the nature of the Lipid-CTA was noticed on both polymerization kinetics and MW control (Fig. S2) in comparison with the good results already reported for NAM homopolymerization.[22] In addition, at the 60/40 NAM/NAS initial molar composition, both monomers copolymerized at the same rate (Table 1), confirming that the copolymerization proceeded at the azeotropic composition. Then, the resulting Lipid-P(NAM-*co*-NAS) copolymers of increasing molecular weight displayed the same composition and microstructure.

Absolute molecular weights (MW) were determined in chloroform (a good solvent for both the lipid and the polymer) by size exclusion chromatography with multi-angle light scattering detection (SEC/MALLS). On the SEC chromatograms, the polymer peak exhibited an apparent trail on the low molecular weight side (Fig. S3). However, this phenomenon was less important in chloroform compared to what was previously observed in THF[22] and did not influence the MW determination thanks to the use of the MALLS detection. Since the MW values remained almost constant along that trail, it suggested the occurrence of some adsorption of the Lipid-P(NAM-*co*-NAS) chains onto the stationary phase of the column due to the lipid chain-end. As shown in Table 1, various LEP samples were synthesized from both **A** and **B** Lipid-CTAs exhibiting MW between 5 900 and 33 000 g.mol^{-1} with low dispersity (Đ) values.

Table 1 Characteristics of the Lipid-P(NAM-*co*-NAS) samples synthesized by RAFT polymerization

Sample[a]	NAM conversion (%)	NAS conversion (%)	M_n (g.mol^{-1})	n_{NAS}[b]	Đ
A1	26	26	7 900	18.1	1.06
A2	59	59	20 300	50.6	1.04
A3	85	85	33 200	84.5	1.11
B1	10	10	5 900	13.1	1.01
B2	83	83	16 600	41.2	1.02

[a] The letter **A** or **B** refers to the type of Lipid-CTA that was used to control the copolymer synthesis

[b] n_{NAS} is the average number of NAS units per polymer chain

We previously showed using MALDI-ToF mass spectrometry that a large majority of the polymer chains retained an intact lipid (coming from the Lipid-CTA) at their α-end.[22] This was further confirmed here by ^{1}H NMR on a low MW conjugate (**B1**, 5 900 g.mol^{-1}) (Fig. 3). Protons corresponding to the lipid-α-chain-end were clearly observed on top of the polymer signals, especially the protons of the fatty acid chains below 1.2 ppm. The more mobile methyl protons at the end of the fatty chains gave a more resolved peak compared to the broad peaks corresponding to the methylene protons. Integrals of these peaks were in agreement with the expected structure. In addition, the characteristic protons

of the dithiobenzoate ω-chain-end were observed at 7.4, 7.6 and 8.0 ppm.

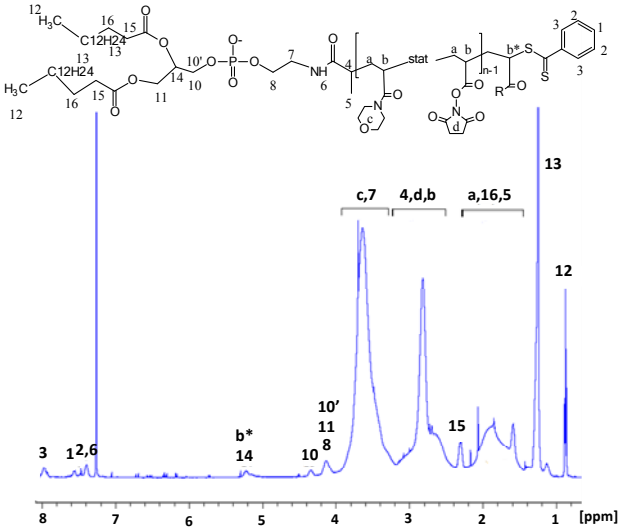

Fig. 3 ^{1}H NMR (500 MHz) spectrum of **B1** LEP in $CDCl_3$

Therefore, the Lipid-copolymers exhibited the following features: i) a controlled and adjustable MW, ii) a narrow MW distribution iii) a lipid at their α-end, iv) multiple activated ester functions regularly spaced along the backbone and available for (bio)conjugation.

Synthesis and characterization of well-defined fluorescent LEPs

Fluorescent LEP conjugates were subsequently elaborated from these multifunctional LEPs using a two-step procedure. The first step consisted in the covalent coupling of a precise number of amino-functionalized chromophores onto the activated ester functions of the NAS units (Fig. 4). Thanks to the well-defined composition of the copolymer chains and to the efficiency of the coupling reaction (60-70% yields were generally obtained) (Table 2), the number of chromophores per polymer chain could be controlled by adjusting the stœchiometry. Then, the second step consisted in a post-treatment of the unreacted activated ester functions along the copolymer chain. On a general point of view, this post-treatment step can be advantageously used to introduce other entities of interest along the backbone but also electrostatic charges. Here, two different post-treatments were performed, either a capping with aminoethylmorpholine (AEM) or a hydrolysis (leading to carboxylate charges) in order to increase the water-solubility and to obtain neutral and negatively charged conjugates, respectively (Fig.4).

A library of fluorescent LEP conjugates was obtained by varying the nature of the lipid at the α-chain-end (from **A** or **B** Lipid-CTAs), the MW of the chains, the average number of chromophores per polymer chain (n_c), and the type of post-treatment of the residual activated ester functions (Table 2). The coupling reaction was evidenced by ^{1}H NMR (Fig. S4) and SEC/UV that was used to monitor the coupling yield and thus n_c (See Experimental section)[39]. Conjugate final MW ranged from 6 800 to 43 100 g.mol^{-1} whereas n_c was varied from 0.7 to 37.8. The average density of chromophores per chain, $d_c = 100 \times n_c / DP_n$ (where DP_n is the average degree of polymerization) was therefore between 0.3 and 17.9%. Finally, the average number of electrostatic charges per chain ranged from 0 for AEM-capped conjugates (except the phosphate charge of the phospholipid) up to 84 carboxylate groups for **A3-1H** hydrolyzed conjugate.

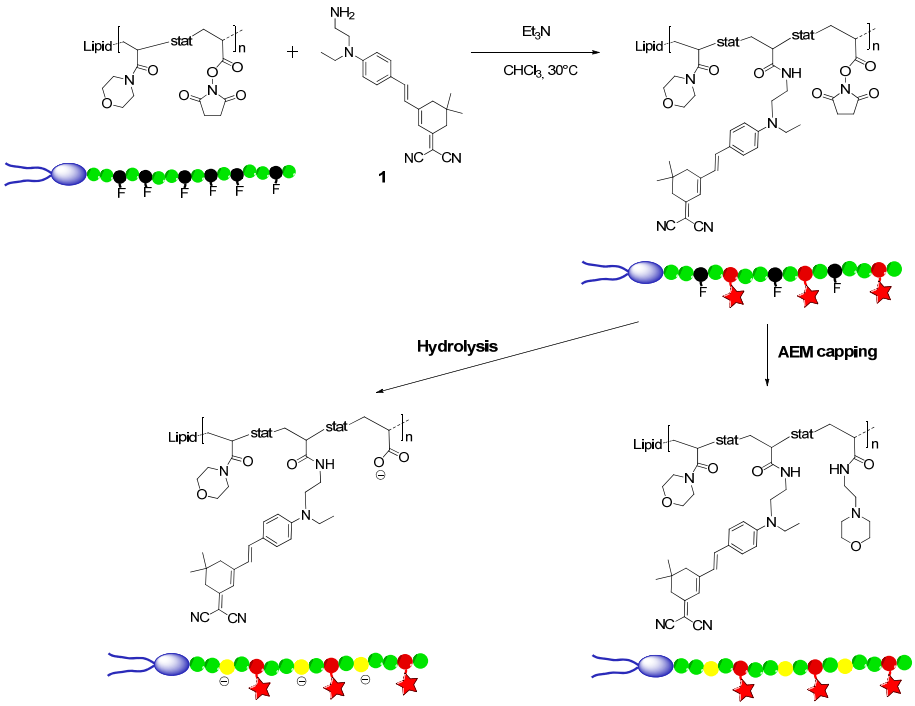

Fig. 4 Covalent coupling of the amino-derivatized chromophore **1** onto the activated lateral functions of the LEPs and post-treatment of the residual reactive functions of the copolymer by either basic hydrolysis or aminoethyl morpholine (AEM) capping

Cite this: DOI: 10.1039/c0xx00000x

www.rsc.org/xxxxxx

ARTICLE TYPE

Table 2 Physico-chemical properties of the fluorescent LEPs

Sample[a]	M_n[b] (g.mol^{-1})	Coupling Yield[c] (%)	n_c[d]	n_{coo-}[e]	d_c[f] (%)
A1-2H	6 800	70	2.0	16.1	4.4
A1-4H	7 500	72	4.1	14.0	9.1
A2-4H	16 800	60	3.8	46.7	3.0
A2-11H	19 200	70	10.8	39.8	8.5
A3-1H	25 500	46	0.7	83.8	0.3
A3-9H	28 300	65	8.5	76.0	4.0
A3-9AEM	36 400	65	8.9	0	4.2
A3-38H	38 000	63	37.8	46.7	17.9
A3-38AEM	43 100	63	37.8	0	17.9
B2-4H	14 000	68	3.9	37.3	3.8

[a] **H** and **AEM** suffixes refer to hydrolyzed and AEM-capped conjugates, respectively

[b] Number average molecular weight of the fluorescent conjugates after post-treatment calculated assuming that the conjugates were in their sodium carboxylate form after dialysis and lyophilization.

[c] Coupling yields determined by SEC/UV[39]

[d] n_c is the average number of chromophores per polymer chain

[e] n_{coo-} is the maximum average number of carboxylate charges per polymer chain. The number of deprotonated COOH groups is variable, depending on the pH and on the distribution of these groups along the polymer backbone.

[f] d_c is the average density of chromophores per polymer chain

For this study, as explained in the Introduction, we used chromophore **1** (Fig. 4) that exhibits the distinctive property to be fluorescent in the crystalline state.[35] Moreover, thanks to several other spectroscopic properties, this fluorophore is particularly well-suited for optical microscopy since it is characterized by i) a large Stokes shift that helps to exclude the scattered and reflected light and to filter background fluorescence[41–43]; ii) a far-red fluorescence emission that fits with the common Cy5 emission filters. However, the free chromophore is hydrophobic and not water-soluble. One of the objectives here was to obtain water-soluble lipid-polymer probes by coupling chromophores **1** onto the Lipid-P(NAM-*co*-NAS) copolymers. This important feature would indeed be an opportunity to enlarge the use of this fluorophore for bioimaging applications.

In fact, the solubility of the fluorescent LEP conjugates depended on d_c and on the type of post-treatment (capping or hydrolysis). Although the free chromophore was water-insoluble, LEP conjugates were soluble in aqueous media, except the conjugate **A3-38AEM** with a very high density of chromophores per chain (d_c = 17.9%). Interestingly, the AEM-capped conjugates were soluble both in water and in chloroform, whereas the hydrolyzed conjugates were soluble in water and in polar organic solvents (such as ethanol and DMF).

Photophysical characterization of the fluorescent LEPs

The direct comparison of the spectroscopic properties of the hydrophobic free chromophore with the corresponding AEM-capped conjugates was possible in the same organic solvent (chloroform). Concerning the hydrolyzed conjugates, their properties were investigated in water (Table 3).

Table 3 Photophysical properties of the fluorescent LEPs

Sample	Solvent	Abs λ_{max} (nm)	Em. λ_{max} (nm)	ε (M^{-1}.cm^{-1})	ϕ[b]	Brightness $\varepsilon\times\phi$
1	$CHCl_3$	505	640	19 000	0.07	1 300
A1-2H	Water	506	688	32 000	0.06	1 900
A1-4H	Water	502	688	58 000	0.03	1 700
A2-4H	Water	508	688	56 000	0.08	4 500
A2-11H	Water	501	691	116 000	0.03	3 500
A3-1H	Water	509	688	12 000	0.10	1 200
A3-9H	Water	501	690	187 000	0.07	13 100
A3-9AEM	$CHCl_3$	505	645	214 000	0.07	15 000
	Water	501	690	231 000	0.02	4 600
A3-38H[a]	Water	503	692	n/a	0.003	n/a
A3-38AEM	$CHCl_3$	502	650	839 000	0.06	50 300
B2-4H	Water	505	689	65 000	0.05	3 100

[a] conjugate poorly soluble in water. It was thus not possible to determine the corresponding extinction coefficient.

[b] measured at λ_{exc} = 510 nm using erythrosin B in MeOH (ϕ_r = 0.09) as the reference.

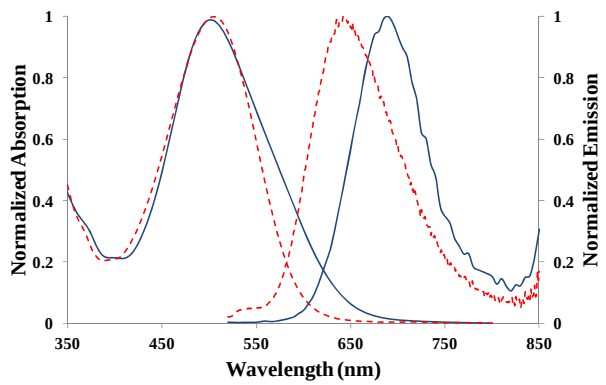

Fig. 5 Absorption and emission spectra of **A3-9AEM** LEP in water (full lines) and in chloroform (dashed lines).

The maximum absorption wavelength of the bound chromophore (≈ 505 nm) remained almost unchanged compared to the free chromophore and was affected neither by the structure of the conjugates nor by the solvent (Fig. S5). Absorption band was slightly broader in water than in chloroform (with a concomitant slight decrease of the extinction coefficient per bound chromophore). In contrast, the fluorescence emission spectrum was clearly red-shifted (by about 50 nm) in water compared to chloroform (due to the increased solvent polarity) (Fig. 5), whatever the structure and post-treatment. The large Stokes shift determined for the conjugates in chloroform (4 430 ± 80 cm^{-1}) was thus even larger in water (5 700 ± 200 cm^{-1}). As expected, fluorescence quantum yield (ϕ) of the bound fluorophore was found to decrease with d_c (Fig. 6) due to fluorescence self-quenching, a well-known phenomenon associated with a high local chromophore concentration.[44] In water, ϕ values were lower

for AEM-capped conjugates compared to hydrolyzed conjugates (ϕ= 0.02 for **A3-9AEM** compared to 0.07 for **A3-9H**) probably reflecting that the hydrolyzed conjugates adopt a more expanded conformation (due to electrostatic repulsions between the carboxylate charges) that disfavors non-fluorescent dimer formation. Nevertheless, AEM-capped conjugates in chloroform and hydrolyzed conjugates (with d_c < 4.5%) in water exhibited ϕ values that were very similar to the one of the free chromophore in chloroform. It has to be mentioned that it is quite exceptional that polymer-chromophore conjugates (especially in water) retain the same fluorescence quantum yield than that of the corresponding free chromophore in organic solvent. Here, it may be due to the unique properties of this chromophore derived from isophorone. Sample **A3-1H**, with on average less than 1 chromophore per chain, was expected to reflect the influence of the binding on the fluorophore properties (de-correlated from the mutual influence of neighboring fluorophores). Its ϕ value of 0.10 was the highest one, indicating a positive influence of the binding onto the polymer chain.

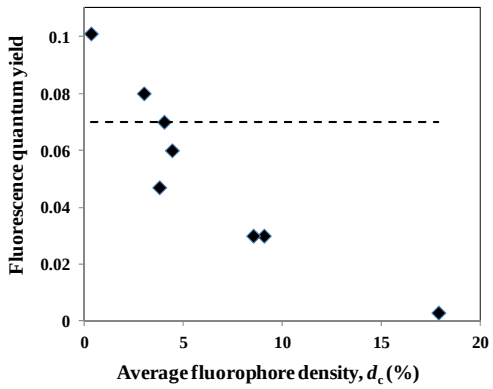

Fig. 6 Fluorescence quantum yield in water versus the average fluorophore density along the polymer chain for the hydrolyzed conjugates. The fluorescence quantum yield of the free chromophore **1** in chloroform is represented as a dashed horizontal line.

Consequently, besides providing water-solubility, multifunctional hydrophilic polymer chains led to far-red emitting conjugates with much improved brightness (B = ε.ϕ) (Table 3). For instance, **A3-38AEM** conjugate was 38 fold brighter in chloroform than the free fluorophore and **A3-9H** conjugate was one order of magnitude brighter in water than the free fluorophore (in chloroform) (Fig. S6).

Labeling of model lipid bi-layers by the fluorescent LEPs

In our previous study, it was shown that lipid-ended P(NAM) homopolymers were able to stabilize LipoParticle assemblies.[22] Here, we used liposomes as model systems in order to test the ability of the fluorescent LEPs to be inserted into lipid bilayers (Fig.7).

Two different approaches were explored by introducing the fluorescent LEP either before or after liposome formation. In the first approach, liposomes of various sizes were prepared from mixtures of natural lipids containing 0.1 and 1 mol% of fluorescent LEPs (e.g. **A3-9H**) using different conventional techniques (Experimental Part). Their sizes were assessed by dynamic light scattering (DLS).

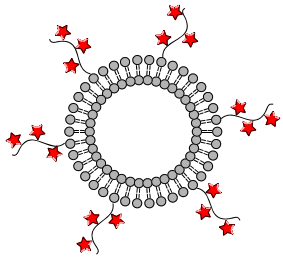

Fig. 7 Schematic representation of liposomes bearing chain-end anchored fluorescent LEPs

First, small unilamellar vesicles (SUVs) were prepared by sonication or extrusion from various lipid mixtures (Table 4). They exhibited a narrow size distribution with diameters as low as 40 nm. The latter was smaller for sonicated vesicles than for extruded ones,[45] and varied with lipid composition. Second, large unilamellar vesicles (LUVs), extruded at 50°C through polycarbonate membranes with controlled porosities (from 50, 100, 200 nm up to 1 µm) gave reproducible results and narrow size distributions (Fig. S7). Nevertheless, their measured diameters (*e.g.* 120 nm for LUV samples extruded through a 100 nm pore-size membrane) were slightly higher than the actual pore size of the membranes. Finally, giant unilamellar vesicles (GUVs) were obtained by electroformation[38] from dioleyl phosphatidylcholine (DOPC) mixtures containing 0.1 mol% of **A3-9H** fluorescent LEP conjugate.[46] They could be observed by optical microscopy since their diameter (> 1µm) was higher than the inherent resolution limit of conventional optical microscopes (> 200 - 400 nm). Using dark-field microscopy, GUVs were visualized as white circles (freely moving in solution) with a 5-10 µm diameter. Fluorescence imaging performed on the same sample confirmed that the GUVs were highly fluorescent in the far-red range in the presence of the LEP conjugate whereas they remained dark in their absence (results not shown). Although the molar concentration of the conjugate into the lipid mixture was very low, the fluorescent GUVs were observed with a high signal-to-noise ratio thanks to the enhanced brightness of the probe.

Table 4 Characteristics of SUVs formed by sonication and extrusion procedures

Composition (mol%)	Preparation	DLS Diameter (nm)
EggPC/PS/LEP[a] 80/20/0.1	Sonication	43
DOPC/C8[b]/LEP[a] 80/20/0.1	Sonication	61
DOPC/DOPE/LEP[a] 75/25/0.1	Sonication	74
DOPC/Chol./LEP[a] 75/25/0.1	Sonication	61
EggPC/PS/LEP[a] 80/20/0.1	Extrusion[c]	95

[a] **A3-9H** conjugate

[b] C8-ceramide

[c] 50 nm pore-size membrane

The second approach was designed to evaluate if the fluorescent LEPs were able to insert into pre-formed liposomes. For this two-step approach, DOPC GUVs were first prepared without conjugate and the absence of fluorescence was confirmed by fluorescence microscopy (Fig. 8, top panels). Then, after incubation of the pre-formed GUVs with an aqueous solution of **A1-2H** LEP conjugate (0.5 mol% compared to DOPC)[47], the GUVs appeared strongly fluorescent, even more than the ones

obtained via the first approach (Fig. 8, low panels).

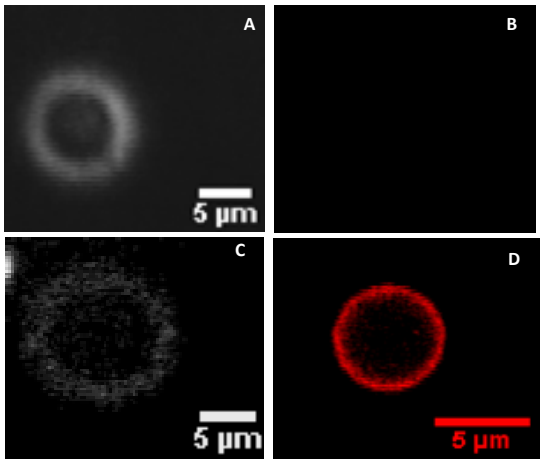

Fig. 8 Dark field (left, A and C) and fluorescence (right, B and D) microscopy images of GUVs obtained by the electroformation process, before (top images, A and B) and after incubation with **A1-2H** LEP conjugate (bottom images, C and D).

Those results confirmed that the fluorescent LEPs were able to insert into lipid bilayers. It is however noteworthy that the intrinsic spatial resolution of fluorescence microscopy is by far not sufficient to firmly affirm that they were anchored in an oriented manner through their lipid α-end. Nevertheless, this assay suggests that the new fluorescent lipid-polymer probes are powerful tools to label the surface of lipid self-assemblies.

Conclusions

The multifunctional lipid-ended polymers, LEPs, reported here constitute a new class of lipid-polymer conjugates (in comparison with lipid-homopolymers like lipid-PEGs), displaying multiple reactive sites regularly distributed along the polymer chains. Their elaboration was based on the synthesis of lipid-functionalized RAFT agents that were successfully used to control the copolymerization of NAM and NAS monomers at the azeotropical composition. The activated ester functions of the resulting Lipid-P(NAM-*co*-NAS) conjugates enable an efficient coupling of a variety of amino-derivatized (bio)-compounds along the polymer backbone.

Here, we developed highly fluorescent LEPs by coupling multiple copies of a far-red emitting chromophore (from 1 to 38) on different Lipid-P(NAM-*co*-NAS) backbones. Although the free fluorophore was not water-soluble, the resulting conjugates were soluble in aqueous media. Their thorough spectroscopic characterization showed that coupling multiple fluorophores along the polymer chain resulted in probes with an enhanced brightness, up to 10 fold in water.

As a first proof of concept, we evidenced that these new fluorescent lipid probes can be inserted into pre-formed lipid bilayers of liposomes of various sizes. Thus, they are very promising tools for the fluorescent labeling of different kinds of lipid self-assemblies. The study of their behavior *in cellulo* will be reported shortly.

More generally, the well-controlled and modular architecture of the multifunctional LEPs that were designed, paved the way towards the elaboration of a large range of functionalized lipid-polymer conjugates. The nature of the lipid, the chain length, the nature of the ω-end group as well as the number and the nature of the bound molecules can be tuned. This modularity thus offers countless opportunities to functionalize the surface of biomimetic lipid membranes, in applications such as liposome-mediated drug delivery.

Experimental section

Materials

All chemicals were purchased from Sigma-Aldrich, Acros and Fluka at the highest purity available and used without further purification. THF and 1,4-dioxane were distilled over $LiAlH_4$. *N*-acryloyl morpholine (NAM) (Aldrich, 97%) was distilled under reduced pressure (120°C; 10 mmHg) to remove inhibitor. *N*-acryloxysuccinimide (NAS) was synthesized as previously described.[27] 2,2'-Azobis(isobutyronitrile) (AIBN) was purified by recrystallization from ethanol. Other solvents were used as received from the supplier without further purification. All solvents used for determination of the photophysical properties were of spectrophotometric grade. Lipids including dipalmitoylphosphoethanolamine (DPPE), phosphatidylcholine (PC), phosphatidylserine (PS), dioleolylphosphocholine (DOPC), C8-Ceramide and cholesterol (Chol) were purchased from Avanti Polar Lipids and Sigma-Aldrich.

Synthesis and purification of Lipid-CTAs

Lipid-functionalized chain transfer agents (Lipid-CTAs) were synthesized from succinimido-2-[[2-phenyl-1-thioxo]thio]-propanoate (SEDB)[36] following the procedure described by Bathfield *et al.*.[22] Purification protocols for both SEDB and the Lipid-CTAs were however improved compared to the original procedure as explained below.

Purification of SEDB. After synthesis of 2-[[2-phenyl-1-thioxo]thio]-propanoic acid (CAEDB), the reaction medium was extracted with a 1M KOH aqueous solution. The aqueous phase was washed three times with chloroform before acidification to pH 2 with HCl and extracted with chloroform. The organic phase was finally washed three times with deionized water, concentrated and subjected to silica gel chromatography (Silica gel 60, Merck) using chloroform/ethyl acetate as eluent (composition was progressively varied from 100 to 80 vol% chloroform), leading to the expected CAEDB red crystalline compound with a >95% purity (^{1}H NMR) (final yield after purification: 45%).

After SEDB synthesis from CAEDB, the reaction mixture was filtrated. After solvent removal, the product was twice dissolved in a minimum volume of ethyl acetate and filtrated. The product was finally purified by re-cristallization in a mixture of chloroform/pentane (10/90 vol%) leading to a pink solid with a >95% purity (^{1}H NMR) (final yield after purification: 35%).

Purification of Lipid-CTAs. After Lipid-CTA synthesis, the reaction mixture was washed three times with a NaCl aqueous solution (100g.L^{-1}). The organic phase was then filtered twice over a small pad of silica gel (Silica gel 60, Merck) using chloroform/ethanol (70/30 vol%) as eluent. Lipid-CTAs were

obtained as pink/red powders (90% yield, >90% purity).

The newly synthesized **B** Lipid-CTA was obtained using this protocol with DPPE as the lipid:
^{1}H NMR 200 MHz ($CDCl_3$, 300K): δ(ppm) : 0,88 (6H) ; 1,24 (48H) ; 1,56 (4H) ; 1,63 (3H) ; 2,26 (4H) ; 3,47 (2H) ; 3,91 (4H) ; 4,10 (1H) ; 4,34 (1H) ; 4,69 (1H) ; 5,18 (1H) ; 7,35 (dd, 2H) ; 7,51 (dd, 2H) ; 7,97 (d, 2H).
ESI-ToF mass spectrometry (microToF QII Bruker Daltonics): Characteristic ion $[M-H]^-$, $C_{47}H_{81}NO_9PS_2$; calculated 898.5090 mass units; found 898.5073 mass units.

Synthesis of multifunctional LEP conjugates

Poly(NAM-*co*-NAS) copolymer synthesis in the presence of the Lipid-CTA was adapted from the procedure previously described for the homopolymerization of NAM.[22] The initial co-monomer molar ratio was the azeotropical composition 60/40 mol% NAM/NAS.
Briefly, NAM (1.112 g, 7.88 mmol), NAS (0.888 g, 5.25 mmol), Lipid-CTA **A** (103.2 mg, 0.115 mmol), AIBN (3.44 mg, 0.021 mmol), dioxane (5.57 mL), and trioxane (0.056 g, internal reference for ^{1}H NMR determination of monomer consumption) were introduced in a Schlenk tube equipped with a magnetic stirrer. The mixture was degassed by 3 freeze-evacuate-thaw cycles and then heated under nitrogen using a thermostated oil bath (80 °C). Periodically, samples were withdrawn from the polymerization medium for analyses. Polymers were precipitated in a large volume of diethyl ether, recovered by centrifugation, and finally dried under vacuum.

Synthesis of fluorescent LEP conjugates

Chromophore coupling. Below is the typical procedure for the coupling of **1** onto the Lipid-P(NAM-*co*-NAS) copolymer **A3**. An identical procedure was used for the synthesis of all fluorescent LEP conjugates.
25 mg of Lipid-P(NAM-*co*-NAS) copolymer were dissolved in 1 mL of chloroform in a 25 mL round bottom flask equipped with a magnetic stirrer. Then, 3.6 mg of **1** dissolved in chloroform (9.7×10^{-2} M) were added together with 2 equivalents of triethylamine (Et_3N). Polymer concentration was adjusted to 10 mg.mL^{-1} with chloroform and the coupling reaction was carried out at 40°C in the dark under stirring for 24 hours. The coupling yield was followed by SEC/UV measurements and was typically between 60-70%. The red LEP conjugate was then precipitated in a large volume of diethyl ether and isolated by centrifugation. The procedure was repeated until complete discoloration of the supernatant, indicatingthe removal of the free unreacted fluorophore. Purified conjugates were finally dried under vacuum up to constant weight.
Post-treatment of residual reactive functions. After chromophores coupling, the residual activated ester units along the polymer chains were either capped with aminoethylmorpholine (AEM) or hydrolyzed.
AEM capping. 25 mg of conjugates were re-dispersed in 3 mL of chloroform before addition of a 10-fold molar excess of AEM (compared to the initial NAS units). The capping reaction proceeded at room temperature under magnetic stirring overnight. The conjugates were then isolated by precipitation in diethyl ether before dialysis against deionized water (Spectrum Labs, Spectra/Por 6, MWCO: 2 kg.mol^{-1}) and finally dried by lyophilization.
Hydrolysis. 45 mL of a borate buffer (50 mM, pH = 9) were added to 25 mg of conjugates. Hydrolysis proceeded at room temperature under magnetic stirring for 3 days. After hydrolysis, conjugates were purified by dialysis against deionized water (Spectrum Labs, Spectra/Por 6, MWCO: 2 kg.mol^{-1}) and dried by lyophilization.

Liposome Model Systems

Large and small unilamellar vesicles, LUVs and SUVs respectively, were prepared by extrusion.[37] Mixtures in water of EggPC (160 µL of a 10 mg.mL^{-1} solution), BrainPS (40 µL of a 10 mg.mL^{-1} solution) (80/20 mass%) and the fluorescent LEP conjugate (0.1 mol% of the total lipids) were dried in a Speedvac rotary evaporator overnight. The dry lipid film was then hydrated with a PBS buffer pH 7.4 for 2 hours at 45°C, with vortexing every 15 minutes. 12 freeze/thaw cycles were performed by freezing the vesicle solutions in liquid nitrogen followed by thawing (water bath, 40°C). These solutions were finally extruded at 50°C, through controlled pore-size polycarbonate membranes (Whatman Nucleopore Track-Etch, 19 mm), using an Avanti Polar Lipids miniextruder.
Small unilamellar vesicles, SUVs, were also prepared by sonication of lipid mixtures in PBS solution (10 mg.mL^{-1}) using a Bioruptor®Plus (UCD-300) from Diagenode. Solutions were maintained at 60°C before sonication (12 × 6 cycles of 1 minute – 320W).
Giant unilamellar vesicles, GUVs, were prepared by electroformation following the procedure described by Portet *et al.*[38] from a 0.5 mg.mL^{-1} chloroform/ethanol 90/10 vol% solution of DOPC containing 0.1 mol% (compared to DOPC) of fluorescent LEP conjugate. To test the ability of the fluorescent LEP conjugates to insert into pre-formed GUVs, 100 mol% DOPC GUVs were first prepared using the above-mentioned procedure, before incubation with an aqueous solution of LEP conjugate (**A1-2H**, 0.5 mol% compared to DOPC) under gentle stirring for 2 hours at 37°C.

Characterization techniques

^{1}H NMR. Spectra were recorded in deuterated chloroform at room temperature (300 K) on a Bruker DPX 200 spectrometer operating at 200.13 MHz and on a Bruker 500 Ultra Shield spectrometer operating at 500.1 MHz. Chemical shifts are reported in ppm with tetramethylsilane as internal standard.
SEC/MALLS. Size exclusion chromatography coupled with multi-angle laser light scattering detection (SEC/MALLS) was performed using a set up composed of a Shimadzu LC-6A liquid chromatography pump and a PLgel Mixed-C column (5µm size pores). Online double detection was provided by a differential refractometer (DRI Waters 410) and a three-angle (46°, 90°, 133°) MiniDAWN TREOS light scattering photometer (Wyatt Technologies), operating at 658 nm. Analyses were performed by injection of 70 µL of polymer solution (5 mg.mL^{-1}) in chloroform. The specific refractive index increment (d_n/d_c) for

Lipid-P(NAM-*co*-NAS) copolymer in the same eluent (0.130 mL.g^{-1}) was previously determined with a NFT ScanRef monocolor interferometer operating at 633 nm. The molar mass and polydispersity data were determined using the Wyatt ASTRA SEC/ LS software package.

SEC/UV. Size exclusion chromatography coupled with UV/Vis detection (SEC/UV) was used to monitor the coupling yield of the fluorophore onto the Lipid-P(NAM-*co*-NAS) copolymers following the previously described procedure.[39] This was performed using a Waters 1515 isocratic HPLC pump (flow rate: 1 mL.min^{-1}) and a Styragel HR4E Waters column (7.8x300 mm²). The eluent was dimethylformamide (DMF) with LiBr (0.05 mol.L^{-1}) at 30°C. Detection was provided by both a Waters 2410 refractive index detector and a Waters 2489 UV-Visible detector set at 488 nm. Analyses were performed by injection of 10 µL of polymer solution (5 mg.mL^{-1}) in DMF. Data acquisition and treatment was performed using the Breeze software.

UV-Visible absorption. Spectra were recorded on a Jasco V-670 spectrophotometer at ambient temperature using 1 cm quartz cells.

Fluorescence emission. Spectra were measured using a Horiba–Jobin Yvon Fluorolog-3® spectrofluorimeter at 298K, using a 1 cm quartz cells. The steady-state luminescence of diluted solutions was excited by unpolarized light from a 450 W xenon CW lamp and detected at right angle (90°) by a red-sensitive Hamamatsu R928 photomultiplier tube. Spectra were reference corrected for both the excitation source light intensity variation (lamp and grating) and the emission spectral response (detector and grating). References were Erythrosin B in MeOH ($\Phi r = 0.09$) at 510 nm and Rubrene in MeOH ($\Phi r = 0.27$) at 488 nm.[40] Both gave similar results. Excitation of reference and sample compounds was performed at the same wavelength.

Dark-field and fluorescence microscopy. Samples were prepared by depositing a drop of GUV solution on a glass coverslip. Imaging was performed at room temperature using an inverted microscope (DM IRBE, LEICA, Germany). A 40X and a 100X oil immersion objectives (LEICA) were used respectively for dark field and fluorescence microscopy. Light source for dark field was a 100 W halogen lamp and for fluorescence microscopy an X-cite 120PCQ (Lumen Dynamics, Canada) coupled to a TX2 bandpass filter (LEICA). Image obtained from an EB-CCD camera (640 × 480 pixels, 14 µm pixel, 8 bit, Hamamatsu, Japan) were converted in TIFF format using Wasabi software (Hamamatsu) and thereafter processed with ImageJ (NIH, USA). The images shown here are representative of the different images obtained during acquisition.

Dynamic light scattering. The sizes of the lipid vesicles (SUVs and LUVs) were measured by DLS, at room temperature, using a Particle Size Analyzer DL 135 from Cordouan Technologies. Solutions of vesicles were diluted 6 times in PBS before deposition of a drop on the measurement cell. The sizes were measured using a 658 nm laser diode at 25°C in continuous mode until stabilization of the value (at least 5 minutes acquisition). The data were treated by NanoQ software.

Acknowledgments

We acknowledge the contribution of Jean-Michel Lucas and Agnès Crépet (Laboratoire d'Ingénierie des Matériaux Polymères) for technical support in SEC/MALLS measurements, Sandrine Denis-Quanquin (Laboratoire de Chimie, ENS de Lyon) for NMR measurements and Elise Hamard-Péron for her help with the liposome extrusion technique. SA acknowledges a PhD grant from the Région Rhône-Alpes, Cluster 5 Chimie. WL was supported by an AMI grant from the French Bioimaging network, GDR 2588 MiFoVI-CNRS. We also thank the Fondation Innovations en Infectiologie, FINOVI, and the CNRS interdisciplinary program (PIR051) for funding.

Notes and references

[a] *École Normale Supérieure de Lyon, Laboratoire Joliot-Curie, CNRS USR3010, F-69364 Lyon, France. E-mail : arnaud.favier@ens-lyon.fr*
[b] *INSA-Lyon, Laboratoire Ingénierie des Matériaux Polymères, CNRS UMR5223, F-69621 Villeurbanne, France.*
[c] *École Normale Supérieure de Lyon, CNRS UMR5182, Université Lyon 1, Site Monod, 46 allée d'Italie, F-69364, Lyon, France.*
[d] *Centre d'études d'agents Pathogènes et Biotechnologies pour la Santé, CNRS UMR5236, F-34293, Montpellier, France*
[e] *École Normale Supérieure de Lyon, Laboratoire de Virologie Humaine, INSERM U758, F-69364 Lyon*

† Electronic Supplementary Information (ESI) available: Complementary physico-chemical and photo-physical characterizations of Lipid-CTAs (^{1}H NMR), multifunctional LEPs (SEC chromatogram, ^{1}H NMR), fluorescent LEPs (Absorption and emission spectra of **A3-9AEM** and chromophore **1** in chloroform, brightness of chloroform-soluble compounds) and liposomes (size distribution measured by DLS for **A3-9H**). See DOI: 10.1039/b000000x/

‡ Present address: *Centre d'études d'agents Pathogènes et Biotechnologies pour la Santé, CNRS UMR5236, F-34293, Montpellier, France*.

1 V. P. Torchilin, *Nat. Rev. Drug Discov.*, 2005, **4**, 145.
2 J. C. Su, C. L. Tseng, T. G. Chang, W. J. Yu and S. K. Wu, *Bioorg. Med. Chem. Lett.*, 2008, **18**, 4593.
3 S. Zalipsky, B. Puntambekar, P. Boulikas, C. M. Engbers and M. C. Woodle, *Bioconjugate Chem.*, 1995, **6**, 705.
4 G. Bendas, A. Krause, U. Bakowsky, J. Vogel and U. Rothe, *Int. J. Pharm.*, 1999, **181**, 79.
5 K. Edwards, M. Johnsson, G. Karlsson and M. Silvander, *Biophys. J.*, 1997, **73**, 258.
6 N. Dos Santos, C. Allen, A. M. Doppen, M. Anantha, K. A. K. Cox, R. C. Gallagher, G. Karlsson, K. Edwards, G. Kenner, L. Samuels, M. S. Webb and M. B. Bally, *Biochim. Biophys. Acta*, 2007, **1768**, 1367.
7 S. Sriwongsitanont and M. Ueno, *Chem. Pharm. Bull.*, 2002, **50**, 1238.
8 A. L. Klibanov, K. Maruyama, V. P. Torchilin and L. Huang, *FEBS Letters,* 1990, **268**, 235.
9 S. Unezaki, K. Maruyama, O. Ishida and A. Suginaka, *Int. J. Pharm.*, 1995, **126**, 41.
10 V. P. Torchilin, T. S. Levchenko, A. N. Lukyanov, B. A. Khaw, A. L. Klibanov, R. Rammohan, G. P. Samokhin and K. R. Whiteman, *Biochim. Biophys. Acta,* 2001, **1511**, 397.
11 S. Zalipsky, *Adv. Drug Deliv. Rev.*, 1995, 16, 157.
12 M. T. Allen, E. Brandeis, C. B. Hansen, G. Y. Kao and S. Zalipsky, *Biochim. Biophys. Acta*, 1995, **1237**, 99.
13 F. Albertorio, A. J. Diaz, T. Yang, V. A. Chapa, S. Kataoka, E. T. Castellana and P. S. Cremer, *Langmuir,* 2005, **21**, 7476.
14 G. A. F. Van Tilborg, E. Vucic, G. J. Strijkers, D. P. Cormode, V. Mani, T. Skajaa, C. P. M. Reutlingsperger, Z.A. Fayad, W. J. M. Mulder and K. Nicolay, *Bioconjugate Chem.*, 2010, **21**, 1794.

15 G. Moad, Y. K. Chong, A. Postma, E. Rizzardo and S. H. Thang, *Polymer*, 2005, ***46***, 8458.
16 A. Favier and M. T. Charreyre, *Macromol. Rapid Commun.*, 2006, **27**, 653.
17 K. Matyjaszewski and J. Xia, *Chem. Rev.,* 2001, **101**, 2921.
18 C. J. Hawker, A. W. Bosman and E. Harth, *Chem. Rev.*, 2001, **101**, 3661.
19 K. Ohno, T. Fukuda and H. Kitano, *Macromol. Chem. Phys.*, 1998, **199**, 2193.
20 H. Götz, E. Harth, S. M. Schiller, C. W. Frank, W. Knoll and C. J. Hawker, *J. Polym. Sci., Part A: Polym. Chem.*, 2002, **40**, 3379.
21 P. Kujawa, F. Segui, S. Shaban, C. Diab, Y. Okada, F. Tanaka and F. M. Winnik, *Macromolecules*, 2006, **39**, 341.
22 M. Bathfield, D. Daviot, F. D'Agosto, R. Spitz, C. Ladavière, M. T. Charreyre and T. Delair, *Macromolecules*, 2008, **41**, 8346.
23 L. Hespel, E. Kaifas, L. Lecamp, L. Picton, G. Morandi and F. Burel, *Polymer*, 2012, **53**, 4344.
24 A. Favier, B. De Lambert and M. T. Charreyre, In *Handbook of Raft Polymerization*; Barner-Kowollik C. Ed.; Wiley-VCH, 2008; p.556.
25 C. A. G. N. Montalbetti and V. Falque, *Tetrahedron*, 2005, **61**, 10827.
26 J. Hwang, R. C. Li and H. D. Maynard, *J. Control. Release*, 2007, **122**, 279.
27 A. Favier, F. D'Agosto, M. T. Charreyre and C. Pichot, *Polymer,* 2004, **45**, 7821.
28 O. Maier, V. Oberle and D. Hoekstra, *Chem. Phys. Lipids,* 2002, **116**, 3.
29 J. A. Monti, S. T. Christian and W. A. Shaw, *J. Lipid Res.*, 1978, **19**, 222.
30 A. Chaudhary, J. Chen, Q. M. Gu, W. Witke, D. J. Kwiatkowski and G. D. Prestwich, *Chem. & Biol.*, 1998, **5**, 273.
31 R. Koynova, H. S. Rosenzweig, L. Wang, M. Wasielewski and R. C. MacDonald, *Chem. Phys. Lipids,* 2004, **129**, 183.
32 W. Qin, D. Ding, J. Liu, W. Z. Yuan, Y. Hu, B. Liu and B. Z. Tang, *Adv. Funct. Mater.*, 2012, **22**, 771.
33 V. Pansare, S. Hejazi, W. Faenza and R. K. Prud'homme, *Chem. Mater.*, 2012, **24**, 812.
34 J. Massin, A. Charaf-Eddin, F. Appaix, Y. Bretonnière, D. Jacquemin, B. Van der Sanden, C. Monnereau and C. Andraud, *Chem. Sci.*, 2013, **4**, 2833.
35 J. Massin, W. Dayoub, C. Mulatier, C. Aronica, Y. Bretonnière and C. Andraud, *Chem. Mater.*, 2011, **23**, 862.
36 M. Bathfield, F. D'Agosto, R. Spitz, M. T. Charreyre and T. Delair, *J. Am. Chem. Soc.*, 2006, **128**, 2546.
37 G. Blin, E. Margeat, K. Carvalho, C. A. Royer, C. Roy and C. Picart, *Biophys. J.*, 2008, **94**, 1021.
38 T. Portet, F.C. i Febrer, J. M. Escoffre, C. Favard, M. P. Rols and D. S. Dean, *Biophys. J.*, 2009, **96**, 4109.
39 C. Cepraga, T. Gallavardin, S. Marotte, P. H. Lanoë, J. C. Mulatier, F. Lerouge, S. Parola, M. Lindgren, P. L. Baldeck, J. Marvel, O. Maury, C. Monnereau, A. Favier, C. Andraud, Y. Leverrier and M. T. Charreyre, *Polym. Chem.*, 2013, **4**, 61.
40 N. Boens, W. Qin, N. Barasić, J. Hofkens, M. Ameloot, J. Pouget, J. P. Lefèvre, B. Valeur, E. Gratton, M. VandeVen, N. D. Jr. Silva, Y. Engelborghs, K. Willaert, A. Sillen, A. J. W. G. Visser, A. Van Hoek, J. R. Lakowicz, H. Malak, I. Gryczynski, A. G. Szabo, D. T. Krajcarski, N. Tami and A. Miura, *Anal. Chem.*, 2007, **79**, 2137.
41 A. J. Amoroso, M. P. Coogan, J. E. Dunne, V. Fernández-Moeira, J. B. Hess, A. J. Hayes, D. Lloyd, C. Millet, S. J. A. Pope and C. Williams, *Chem. Commun.*, 2007, 3066.
42 A. N. Glazer, *J. Appl. Phyco.,* 1994, **6**, 105.
43 K. D. Piatkevich, J. Hulit, O. M. Subach, A. Abdulla, J. E. Segall and V. V. Verkhusha, *Proc. Natl. Acad. Sci.*, 2010, **107**, 5369.
44 J. Baumann and M. D. Fayer, *J. Chem. Phys.*, 1986, **85**, 4087.
45 L. T. Boni, M. M. Batenjany, M. E. Neville, Y. Guo, L. Xu, F. Wu, J. T. Mason, R. J. Robb and M.C. Popescu, *Biochim. Biophys. Acta*, 2001, **1514**, 127.
46 Y. Yamashita, M. Oka, T. Tanaka and M. Yamazaki, *Biochim. Biophys. Acta*, 2002, **1561**, 129.
47 D. Cuvelier, C. Vezy, A. Viallat, P. Bassereau and P. Nassoy, *J. Phys. : Condens. Matter*, 2004, **16**, S2427.